AD-A153 152 LABORATORY MODELING OF ASPECTS OF LARGE FIRES(U) TRW 1/1
ELECTRONICS AND DEFENSE SECTOR REDONDO BEACH CA
G F CARRIER ET AL. 30 APR 84 TRW-42504-6001-UT-00
UNCLASSIFIED DNA-TR-84-18 DNA001-83-C-0228 F/G 13/12 NL

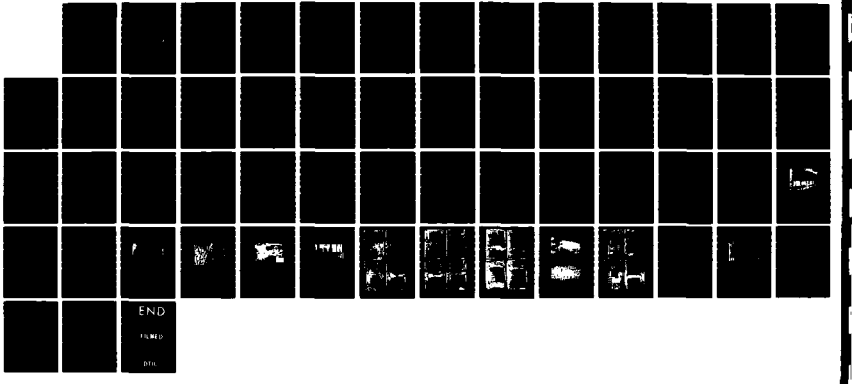

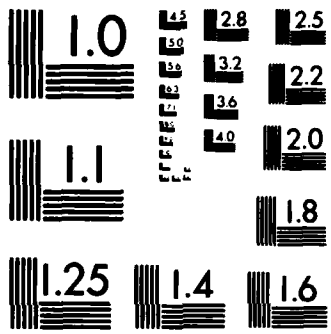

PHOTOGRAPH THIS SHEET

AD-A153 152

DTIC ACCESSION NUMBER

III

LEVEL

1

INVENTORY

DNA-TR-84-18

DOCUMENT IDENTIFICATION

30 April 1984

DISTRIBUTION STATEMENT A
Approved for public release;
Distribution Unlimited

DISTRIBUTION STATEMENT

ACCESSION FOR	
NTIS GRA&I	☒
DTIC TAB	☐
UNANNOUNCED	☐
JUSTIFICATION	
BY	
DISTRIBUTION /	
AVAILABILITY CODES	
DIST	AVAIL AND/OR SPECIAL
A-1	

DISTRIBUTION STAMP

DTIC COPY INSPECTED 1

DTIC
ELECTE
MAY 2 1985
S D
D

DATE ACCESSIONED

DATE RETURNED

85 05 01 041

DATE RECEIVED IN DTIC

REGISTERED OR CERTIFIED NO.

PHOTOGRAPH THIS SHEET AND RETURN TO DTIC-DDAC

DTIC FORM 70A DEC 83

DOCUMENT PROCESSING SHEET

PREVIOUS EDITION MAY BE USED UNTIL STOCK IS EXHAUSTED.

DNA-TR-84-18

LABORATORY MODELING OF ASPECTS OF LARGE FIRES

G.F. Carrier
F.E. Fendell
R.D. Fleeter
N. Gat
L.M. Cohen
TRW Electronics & Defense Sector
One Space Park
Redondo Beach, CA 90278

30 April 1984

Technical Report

CONTRACT No. DNA 001-83-C-0228

APPROVED FOR PUBLIC RELEASE;
DISTRIBUTION UNLIMITED.

THIS WORK WAS SPONSORED BY THE DEFENSE NUCLEAR AGENCY
UNDER RDT&E RMSS CODE B345083466 G54CMXGD00001 H2590D.

Prepared for

Director
DEFENSE NUCLEAR AGENCY
Washington, DC 20305

Destroy this report when it is no longer needed. Do not return to sender.

PLEASE NOTIFY THE DEFENSE NUCLEAR AGENCY, ATTN: STTI, WASHINGTON, D.C. 20305, IF YOUR ADDRESS IS INCORRECT, IF YOU WISH TO BE DELETED FROM THE DISTRIBUTION LIST, OR IF THE ADDRESSEE IS NO LONGER EMPLOYED BY YOUR ORGANIZATION.

UNCLASSIFIED

SECURITY CLASSIFICATION OF THIS PAGE

REPORT DOCUMENTATION PAGE

1a. REPORT SECURITY CLASSIFICATION UNCLASSIFIED	1b. RESTRICTIVE MARKINGS
2a. SECURITY CLASSIFICATION AUTHORITY	3 DISTRIBUTION / AVAILABILITY OF REPORT Approved for public release; distribution unlimited.
2b. DECLASSIFICATION / DOWNGRADING SCHEDULE	
4. PERFORMING ORGANIZATION REPORT NUMBER(S) 42504-6001-UT-00	5. MONITORING ORGANIZATION REPORT NUMBER(S) DNA-TR-84-18
6a. NAME OF PERFORMING ORGANIZATION TRW Electronics & Defense Sector 6b. OFFICE SYMBOL (If applicable)	7a. NAME OF MONITORING ORGANIZATION Director Defense Nuclear Agency
6c. ADDRESS (City, State, and ZIP Code) One Space Park Redondo Beach, California 90278	7b. ADDRESS (City, State, and ZIP Code) Washington, DC 20305
8a. NAME OF FUNDING / SPONSORING ORGANIZATION 8b OFFICE SYMBOL (If applicable)	9 PROCUREMENT INSTRUMENT IDENTIFICATION NUMBER DNA 001-83-C-0228
8c. ADDRESS (City, State, and ZIP Code)	10. SOURCE OF FUNDING NUMBERS PROGRAM ELEMENT NO: 62715H; PROJECT NO: G54CMXG; TASK NO: D; WORK UNIT ACCESSION NO: DH006945

11 TITLE (Include Security Classification)

LABORATORY MODELING OF ASPECTS OF LARGE FIRES

12. PERSONAL AUTHOR(S) G.F. Carrier, F.E. Fendell, R.D. Fleeter, N. Gat, L.M. Cohen

13a. TYPE OF REPORT	13b. TIME COVERED	14. DATE OF REPORT (Year, Month, Day)	15. PAGE COUNT
Technical Report	FROM 83Jun14 TO 84Apr30	1984 April 30	56

16. SUPPLEMENTARY NOTATION

This work was sponsored by the Defense Nuclear Agency under RDT&E RMSS Code B345083466 G54CMXGD00001 H2590D.

17 COSATI CODES			18. SUBJECT TERMS (Continue on reverse if necessary and identify by block number)
FIELD	GROUP	SUB-GROUP	Buoyant Plume; Fire Spread; Fire; Nuclear Weapons Effects
13	12		
14	2		

19. ABSTRACT (Continue on reverse if necessary and identify by block number)

The design, construction, and use of a laboratory-scale combustion tunnel for simulating aspects of large-scale free-burning fires are described. The facility consists of an enclosed, rectangular-cross section (1.12 m wide x 1.27 m high) test section of about 5.6 m in length, fitted with large sidewall windows for viewing. A long upwind section permits smoothing (by screens and honeycombs) of a forced-convective flow, generated by a fan and adjustable in wind speed (up to a maximum speed of about 20 m/s prior to smoothing). Special provision is made for unconstrained ascent of a strongly buoyant plume, the duct over the test section being about 7 m in height. Also, a translatable test-section ceiling can be used to prevent jet-type spreading into the duct of the impressed flow; that is, the wind arriving at a site (say) half-way along the test section can be made (by ceiling movement) approximately the same as that at the leading edge of the test section with a fully open duct (fully retracted ceiling). Of particular interest here are the rate and structure of wind-aided flame spread streamwise along a uniform matrix of vertically oriented small fuel elements (such as toothpicks or

20. DISTRIBUTION / AVAILABILITY OF ABSTRACT ☐ UNCLASSIFIED/UNLIMITED ☒ SAME AS RPT. ☐ DTIC USERS	21. ABSTRACT SECURITY CLASSIFICATION UNCLASSIFIED
22a. NAME OF RESPONSIBLE INDIVIDUAL Betty L. Fox	22b. TELEPHONE (Include Area Code) (202)325-7042 22c. OFFICE SYMBOL DNA/STTI

DD FORM 1473, 84 MAR

83 APR edition may be used until exhausted.
All other editions are obsolete.

SECURITY CLASSIFICATION OF THIS PAGE
UNCLASSIFIED

19. ABSTRACT (Continued)

coffee-stirrers), implanted in clay stratum on the test-section floor; this experiment is motivated by flame spread across strewn debris, such as may be anticipated in an urban environment after severe blast damage. However, the experiment can be readily modified to examine flame spread against the wind, flame spread without ambient wind, and minimum width of firebreaks precluding nonspotting spread. Further, the facility itself can be modified to examine the mechanism(s) for enhanced entrainment into the flaming, low-level, strongly buoyant portion of the convective plume associated with intense nonpropagating fire.

PREFACE

The authors wish to thank Michael Frankel, the technical monitor, for the opportunity to pursue this investigation; they are also grateful for assistance from Robert Flory and Ralph Wege. The participation of technicians Frank Farey, Kurt Hoover, Shuzo Sakurai, and Richard Yee is also acknowledged. Finally, the authors are indebted to Ann McCollum for preparation of the manuscript and to Asenatha McCauley for preparation of the figures.

TABLE OF CONTENTS

LIST OF ILLUSTRATIONS

1. INTRODUCTION

1.1 Incendiary Effects of Thermonuclear Events in Urban Environments

Relative to the attention devoted to blast effects and radioactive-material deposition in the aftermath of a thermonuclear event in an urban environment, little attention has been devoted to the incendiary consequences of nuclear weapons (Glasstone & Dolan 1977). However, it does seem possible, perhaps even plausible, that merger of burning from multiple ignitions, in the strewn debris of a heavily fuel-laden, severely blasted urban environment, could produce large-area fires. These fires might constitute the primary effect of nuclear weapons over most of the urban area involved; as an explicit rough guess, any area exposed to a peak overpressure less than 150 mb or so might be altered primarily by incendiary effects.

Elsewhere it has been conjectured that a large-area fire evolves on the time scale of an hour or so after the nuclear event; the associated convective plume could reach exceptional height [normally, still within the troposphere (Carrier et al 1984a)]. Experience suggests that there are two particular mesoscale atsmopheric conditions prevailing at the time and site of the nuclear event that would have a noteworthy effect on the nature of the fire (Carrier et al 1984b). Interestingly, moderate fallen or falling precipitation seems not to be totally critical, according to experience from massive incendiary-bombing raids conducted on German (Brunswig 1982), English (FitzGibbon 1957) and Japanese (Cate and Craven 1953) cities during World War II, and later on Korean cities (Futrell et al 1961): fire consequences were about as severe, for comparably executed bombing, whether it was raining or not (Broido 1960), and the most severe firestorm (Dresden, Germany, February 1945) occurred during stormy midwinter (Irving 1965). Rather, existence of a sustained wind (significant in magnitude, fairly constant in direction) can lead to rapid fire spread beyond the area of original ignitions (e.g., Tokyo, Japan, April 1945) (Caidin 1960), such that only decay of the wind, exhaustion of fuel, or major prolonged precipitation terminates the flame propagation. Such windy (and dry) conditions are not perennial in most cities, but such occasionally arising conditions do characterize almost all the nonmilitary large urban (and wildland) fire events

historically recorded (Pyne 1982). The other pertinent (significantly rarer) prevailing atmospheric condition at the time and site of multiple ignitions entails a different type of wind, specifically, a well-defined mesoscale cyclone; the convectively induced advection from chemical exothermicity can enhance the role of conservation of angular momentum. From the modest preexisting cyclone, on the time scale of an hour or two, a severe vortical storm (firestorm) can ensue (e.g., Hamburg, Germany, July 1945; Dresden, Germany, February 1945; Hiroshima, Japan, August 1945) (Carrier et al 1983, and references cited therein).

1.2 Motivations for Laboratory-Scale Experiments on Free Burning

Prediction of incendiary consequences of a thermonuclear event, given all the relevant meteorological, topographical, and fuel-property data, must be based on so-called hydrocodes. In turn, validation of such hydrocode calculations must be based on comparison with results of smaller-scale experiments, since urban-scale tests are not feasible. Of course, smaller-scale tests almost assuredly do not permit all relevant physical phenomena of the urban-scale fire to be perfectly replicated. Thus, such tests can furnish but a partial (though still relevant and meaningful) challenge to hydrocodes. More specifically, laboratory-scale tests normally do not permit replication of the roles that (for example) radiative transfer and atmospheric stability play in urban-scale fire. Nevertheless, turbulent burning (in a well-controlled impressed wind under well-characterized thermodynamic conditions of a well-described fuel distribution) permits preliminary verification of a hydrocode over a wide parametric range.

In the absence of complete validation of incendiary-effects-predicting hydrocodes, a role remains for engineering judgment in accepting results. The role left to engineering judgment can be reduced if the partial validation afforded by laboratory-scale tests is supplemented by larger-scale field tests, as in wildlands. Experimental burns in grasslands or in forest stands are invariably fewer in number and less completely instrumented, and involve less completely characterized fuels and less completely controlled ambient conditions. Still, proceeding to larger scale can ascribe hydrocodes with further creditability.

In line with these introductory remarks, attention is focused here on the design, construction, and use of a laboratory-scale facility for experiments on fire spread across a floor-situated matrix of discrete fuel elements, either with an impressed wind, against an impressed wind, or in the absence of an impressed wind. While there are many properties of an observed flame propagation with which to test a theoretical model, including the thickness of the fire front, clearly the key quantity of interest is the rate of fire spread--which for convenience might attain (after decay of starting transients) a quasisteady value in a well-designed experiment.

Further, fire spread with the wind usually far exceeds fire spread against or without a wind, since the wind (by one mechanism or another) tends to abet preheating of uninvolved downwind fuel to its pyrolysis condition (Carrier et al 1984a). Thus, within the more general focus stated in the last paragraph, particular attention is to be paid below to the pertinence of the laboratory facility for wind-aided fire spread.

The above discussion has centered on the usefulness of carrying out laboratory-scale fire-spread experiments through two-dimensional discrete-fuel-element matrices as a means of initiating the validation of hydrocodes. Of course, not all hydrocodes aspire to describe spatial and temporal evolution of a fire from given initial conditions, boundary constraints, and input data (topographical, meteorological, fuel-related, etc.). Less fundamental, special-purpose hydrocodes also may be developed. These might adopt experimental data (perhaps interpreted in terms of dimensionless parameters) as empirical input; for example, a hydrocode may be developed for a Lagrangian-type tracking of the (say, wind-aided) translation in time of a fire front, such that its position at some later time could be inferred from knowledge of its position at some earlier time. (The fire front is a locus, and such a calculation does not involve either fluid-particle or fuel-element tracking in any sense.) Current computer storage-access, processing-speed, and graphical-display capacity is so advanced that the greatest impediment to realization of such a code is physically correct input on fire velocity: at what speed (in a direction perpendicular to the local tangent to the current fire locus) does the fire propagate? Under the plausible quasisteady approximation

that only the instantaneous magnitude of the wind locally perpendicular to the current front is of relevance to wind-aiding, then data from the laboratory flame-spread experiment could furnish the necessary input. Parenthetically, it may be noted that the component of wind perpendicular to the front at the flanks of a fire tends to be small relative to that at the head, and so a constantly elongated elliptical shape tends to evolve for the fire-front configuration under a wind of constant direction--especially since the speed of fire propagation may be relatively negligible not only against the wind but also in the absence of an aiding wind.

Finally, for at least some indication that the facility under discussion does possess flexibility and can be modified readily for practically important fire-dynamic phenomena other than flame spread, a concluding section of this report briefly suggests two other uses. One use concerns identification and quantification of the physical mechanism by which the induction of ambient air into the buoyant plume over an intense fire is augmented at low levels (Carrier et al 1984b). Specifically, it is well documented that the entrainment of air into the strongly buoyant, flaming, low-level region of a buoyant plume exceeds the entrainment into the weakly buoyant, high-level region above the completion-of-burning plane (Cox and Chitty 1980). For the weakly buoyant region, the time-averaged entrainment at the plume edge is found to be linearly proportional (via a rather universal constant) to the time-averaged upflux at the plume axis of symmetry (Morton, Taylor, and Turner 1945). Identification of a comparably general, simplistic, and accurate entrainment "law" near the fire base remains a potentially useful objective of current research in fire science.

2. LABORATORY EXPERIMENTS ON WIND-AIDED FIRE SPREAD ALONG MATRICES OF DISCRETE FUEL ELEMENTS

2.1 Some Basic Concepts

The goal is to achieve a steady one-dimensional flame spread (if one exists) across a two-dimensional array of discrete fuel elements. Such a fuel matrix is to simulate strewn debris; however, a well-defined array (as distinct from a randomly scattered distribution of combustibles) permits reproducibility, and thus a check on the repeatability of the results. Although other cases are introduced, wind-aided spread is of prime interest.

In the presence of an (on time average) uniform and constant impressed wind of known speed and turbulence properties, and in a direction nominally perpendicular to all the elements in every row, one may examine wind-aided fire spread by simultaneously igniting all the fuel elements in the leading (furthest upstream) row, and fire spread against the wind by simultaneously igniting all the elements in the trailing (furthest downstream) row. One has several options for (the not here further discussed case of) flame spread in the absence of a wind; one option is igniting all the elements within a centrally sited circle, though in this case the one-dimensionality would be of cylindrical, rather than Cartesian, character.

While the primary interest is in trying to achieve a steady one-dimensional spread (since such a result would furnish a simple way of characterizing a given experimental test), later one may wish to examine a two-dimensional spread by initially igniting only some of the elements in the "starting" row. In particular, if one ignites just the central elements, one could study the progress of a fire head in the wind-aided context. Particular emphasis on spread at the flank of a fire could be arranged by igniting (say) the entire left half (only) of the starting row.

For the steady one-dimensional spread sought, one must have enough rows in the matrix for initial transients to decay. In fact, the number of rows should be, at the very least, one-and-one-half times the number of rows in the propagating "wave structure," which consists of a preheat zone, a vigorously burning zone

of intense flaming and buoyant convection, and a residual-fuel burn-out zone which may entail heterogeneous oxidation of char [for the synthetic polymers (plastics) and natural polymers (woods) constituting the fuels of interest, because of their use in modern urban construction]. Actually, the thickness of the propagating "wave structure" may be anticipated to be highly variable: for close spacing of thick elements in a high wind, burn-out should occur only long after flame passage and a thick front may be anticipated (especially for relatively tall elements); on the other hand, for widely spaced, thin elements in a modest wind, the elements should burn more individually, and a thinner wave structure may be anticipated. In either case, it is expected that the fuel-loading never reaches such an excess that oxygen-starved burning arises.

The reason that oxygen-starved burning even is mentioned is that the burning of the fuel matrix takes place in an enclosure (provided with large sidewall windows for viewing) to protect against extraneous draughts and to retain the heat of combustion. That is, symmetry conditions associated with noncatalytic, adiabatic sidewalls assist in maintaining the one-dimensionality of the wind-aided and wind-opposed experiments. While zero-perpendicular-derivative wall constraint holds for the thermal and mass-fraction fields, no such constraint holds for the velocity field. Thus, turbulent boundary layers grow with downwind distance on the sidewalls, and it serves no purpose to extend the width of the fuel matrices such that these sidewall boundary layers are entered. Indeed, release of chemical heat too close to the walls threatens the survivability of the glass windows of the sidewalls. Thus, the duct must be taken wide enough that a one-dimensional spread can be maintained in the core of the matrix even for a lengthy array--and even under the constraint that a fuel-free buffer exists between fuel matrix and sidewall window.

Any boundary layer formed on the floor of the test section by the impressed flow replicates a part of the phenomenon of interest. Attention is turned to the ceiling of the test section. At the flaming front of a propagating fire there is strongly buoyant convection, and there should be no ceiling to constrain the ascent of hot gas; for an intense line source of exothermicity, the oncoming impressed flow is diverted vertically upward by the convection, so there is no ambient wind reaching the downwind uninvolved fuel for a one-dimensional spread.

Hence, on these scores one can dispense with a ceiling. On the other hand, forced-convective wind passing over the upstreammost row would expand immediately into the duct; such jet-type spreading implies deceleration, and the flow arriving at a row (say) halfway down the matrix would be of appreciably slower speed than the flow arriving at the upstreammost row. With the impressed flow arriving at every row being different, the attainment of a steady fire propagation is not to be expected. Hence, on this score one requires a ceiling that maintains the flow arriving at the flaming front. The resolution of these requirements is to have a translatable ceiling that may be maintained in position just behind the fire front as that front propagates along the fuel matrix; however, the leading edge of the ceiling should not be advanced downwind so quickly that the ceiling interferes with the strongly buoyant convection occurring at the flaming front.

Radiative transfer cannot play as large a role in laboratory-scale flame spread as it plays in field-scale spread. One might implant radiative sources to give some indication of the effect.

In field experiments gustiness of the wind may result in the buoyant plume being temporarily blown over, because a balance between updraft and crosswind is upset. In the laboratory experiment, it is anticipated that the impressed wind is held constant in magnitude and no such intermittent "flattening" of the convective plume occurs.

However, one aspect of the field event that may warrant replication in the laboratory concerns the presence of an inert mass (in the fuel matrix) that serves as a heat repository. For example, very thick-diameter woody matter (as the tree bole) may serve as a heat sink that does not contribute combustible vapor as the flaming front consumes the thinner-diameter fuels during its passage; indeed, the thick-diameter fuels may not pyrolyze even in the burn-up zone well behind the propagation front. Similarly, different fuel elements in the test matrix could consist of different fuel sizes or--more likely--each fuel element in the matrix might include some inert material.

Finally, it is anticipated that details of the matrix porosity may not be crucial. If one doubles the number of fuel elements by halving the combustible

mass in each element, such that the total mass is held constant, the rate of flame propagation may not be altered much.

2.2 Dimensional Analysis

Instead of the pedantic exercise of trying to list every possible relevant dimensionless group, attention is turned immediately to isolating that subset of groups to which results are anticipated to be most sensitive. For steady one-dimensional wind-aided spread through thermally thin fuel (so that the density, heat capacity, and thermal conductivity of each fuel element can be omitted), in the absence of external radiative sources, the ratio of the steady flame-spread speed v to the uniform wind speed u is taken as a function of ten groups:

$$\frac{v}{u} = f\left[\frac{us}{D}, \frac{u^2}{gs}, \frac{\rho_a c_p T_a s}{Q\sigma}, \phi, \frac{h}{s}, \frac{q}{Q}, \frac{T_l}{T_a}, \gamma, as, \frac{k_f s}{u}\exp\left(-\frac{\theta}{T_a}\right)\right]. \quad (2.1)$$

The total length and width of the matrix are not present, nor is the Stefan-Boltzmann constant of radiative transfer. In fact, some of the ten groups are discarded in the discussion that now follows.

The Peclet number (us/D) involves the separation between fuel elements s and the mass transfer coefficient D (based on ambient conditions: air density ρ_a, air temperature T_a, water-vapor density ρ_v). The dependence on the Peclet number is probably small except as $u \to 0$, such that (D/s) becomes a plausible normalizing speed. This limit seems of minor significance to a wind-aided experiment. The other dynamics-concerned group, the inverse of the Froude number, which entails the magnitude of the gravitational acceleration g, is of significance.

The next parameter, the inverse of the second Damköhler number, which entails the specific heat capacity of air c_p, the exothermicity per mass of fuel Q, and the fuel loading (mass of fuel per area of fuel matrix)σ, also seems of significance. It has been argued elsewhere (Taylor, 1961; Carrier et al 1984a) that the interaction of the crosswind with the buoyant-plume updraft is central to the rate of spread; if convection dynamics (not details of fuel loading)

is central, then the second and third dimensionless groups may be multiplied to eliminate the spacing s. In fact, it has been argued (Carrier et al 1984a), on the basis of a detailed physical model, that linear dependence on the product is relevant:

$$\frac{v}{u} = \frac{\rho_a c_p T_a u^2}{gQ\sigma} F\left[\phi, \frac{h}{s}, \frac{q}{Q}, \frac{T_1}{T_a}, Y\right] . \qquad (2.2)^*$$

Actually the statement is equivalent to the introduction of a group employed by Rouse (1947) on the basis of dimensional arguments. Two further parameters have been omitted in proceeding from (2.1) to (2.2): one involves the radiative absorption coefficient of the burning gases, a; the other is the so-called first Damköhler similarity group $k_f[\exp(-\theta/T_b]/(u/s)$, the ratio of a chemical-reaction rate to a convective-transport rate, such that the group is indefinitely large in chemical equilibrium and effectively zero in chemically nonreacting flow. The factor k_f is the frequency factor, the factor θ is the Arrhenius activation temperature, and the factor T_b is the adiabatic flame temperature. The small role of radiative transfer, relative to convective and diffusive transfer of heat, in laboratory-scale apparati has been noted already. Here it is added that conditions of forced-convective extinction of combustion are of no interest; aside from delineating domains of flame propagation, the first Damköhler number is of little consequence, since it is the rate of spread of well-established burning that is of concern.

*If the specific exothermicity Q were ajusted to account for desiccation and pyrolysis, then it has been suggested (Carrier et al 1984a) that (2.2) might be approximated by the relation

$$\frac{v}{u} = \frac{\rho_a c_p T_a u^2}{8\alpha^2 g Q \sigma} \qquad (2.3)$$

where nominally the Taylor entrainment constant $\alpha \doteq 0.16$. However, this value (inferred on the basis of a Boussinesq approximation) may be an overestimate for hot plumes, and perhaps α should be replaced by $(\rho_p/\rho_a)^{\frac{1}{2}}\alpha$, where subscript p denotes plume. Letting $(\rho_p/\rho_a)^{\frac{1}{2}} \doteq (2/3)$ seems roughly reasonable.

The dimensionless parameters that remain involve h, the thickness of the fuel element (an indicator of the preheating requirements, and of the persistence of burning upon ignition); ϕ, the fuel-matrix porosity, i.e., the ratio of the effective width of fuel elements to the separation s between elements; q, the heat of pyrolyzation per unit mass of the gasifying portion of the fuel [so that (q/Q) is akin to the Spalding B number]; T_1, the temperature at which onset of pyrolysis occurs; and Y, the ratio of the mass of moisture content of a fuel element to its oven-dry mass. It may be appended that the heat of combustion per mass of fuel, Q, does not vary enormously for polymers of interest. Also, since the progress of the flame front is of interest, parameters related to char formation, char erosion, and char oxidation do not seem of central importance.

In summary, validation of the relation $v \alpha u^3/\sigma$ seems one of the most crucial results to be sought from experiment.

3. TEST FACILITY

3.1 Test-Section Sizing

Initial dimensioning of the facility was motivated by the requirement to attain steady flame propagation under wind-aided conditions. After selection of an airflow of minimum sufficient velocity, the rate of flame spread may be estimated. The selection of the test-section length is then based on the criterion of minimum test duration and fuel-element burning time. A test duration of 10-20 seconds is necessary to allow steady-state conditions to be established. Since the objective of the program is to observe propagation of a flame front, the test section must be long compared to the width of this front. The front width is determined by the propagation rate and the burning duration of an individual fuel element.

In the wind-aided mode the momenta of the crosswind and of the thermal plume are approximately matched. The plume buoyancy force F_b is given by

$$F_b = g(\rho_a - \rho_p)hwd, \tag{3.1}$$

where g is the magnitude of the gravitational acceleration, ρ_a and ρ_p the air density at ambient and plume (hot) conditions, respectively; and h,w and d are the plume height, width (crossflow) and depth (streamwise), respectively. The dynamic head of the oncoming flow pushes on the plume with force F_p, where

$$F_p = \rho_a u^2 hw/2, \tag{3.2}$$

where u is the wind speed. If it is taken that the density varies as the inverse of temperature (isobaric conditions) and that the plume temperature is much greater than ambient so that $\rho_p << \rho_a$, the ratio R of the buoyancy to inertia (or inverse of the Froude number) is given by

$$R = 2gd/u^2. \tag{3.3}$$

For equilibration of buoyant and dynamic forces, R is set equal to unity. Then, for a plume thickness d of 1 m, u is 4.5 m/s (9.4 mi/h). Fire

propagation is anticipated to be about an order of magnitude slower than the wind speed, or roughly 50 cm/s for these conditions. For a test duration of ten seconds, a test section of 5 m is required.

Inevitably a test section of 5 m length at wind speeds of about 5 m/s is burdened with thick wall boundary layers. With rough-wall (fully tripped) boundaries, boundary-layer thickness of 20 cm is likely at the end of the 5 m section. The two wall layers will thus reduce the width available for flame propagation without boundary-layer interference by 40 cm. A 1 m tunnel width is selected to allow an undisturbed flow 60 cm in width. At this scaling, fuel-element separation would be about 1 cm to allow a large number of columns of elements. The height of an individual element may be about 5 cm. The flame may extend to ten times the height of the element, or to 50 cm. For a clear view of the flame and at least a portion of the plume above it, a test section height of 1 m is required.

The final tunnel design specifications derived from these considerations is summarized in table 1.

TABLE 1: Fire Tunnel Design Specifications

• Test-section length	5.0 m
• Test-section width	1.1 m
• Test-section height	1.1 m
• Wind speed	0 - 15 m/s

3.2 Thermal-Plume Accommodation

Several other design considerations were made to permit the thermal-plume ascent to be undisturbed. The tunnel is designed without a fixed ceiling on the test section. Instead, a large exhaust hood, equal in width and length to the test section and 2 m high, is fitted to the tunnel. Beginning 3 m above the fuel bed, the hood begins to taper longitudinally to roughly 2 m length, with the width maintained equal to that of the test section. While this arrangement allows the plume to rise, the forced-convective flow tends to turn upward out the exhaust, and not to present a uniform wind to the burning region. A sliding ceiling is provided;

it is pulled over the test section during flame propagation. The leading edge of the ceiling is kept just behind the flame front as the fire proceeds downwind. In this way parallel flow is maintained up to the flame front. Because the leading edge of the ceiling is kept always slightly behind the flame front, the plume is not driven into a horizontal position, but rather is allowed to find a balance between its own momentum and that of the wind.

The blower providing the air supply of the tunnel is upstream of the test section. A downwind blower (suction) is avoided, as it would destroy any reverse flow into the burning region from the downwind side, should the plume block a large portion of the flow area. Figure 3-1 shows the tunnel schematically and figure 3-2 is a photograph of the installed assembly.

3.3 Structural and Thermal Design

The tunnel was designed to accommodate large transient heat loads and to be free from vibration from either the blower or air turbulence. At the highest anticipated fuel loading (about 5 g/cm^2) approximately 50 kg of fuel could be consumed in one minute, with heat release at a rate of almost 17 kW. The tunnel is constructed of eleven identical frame sections constructed of 6.4 mm (0.25 in) thick aluminum. The frames are bolted together, with separation by high-temperature silicon-rubber gaskets. This provision allows thermal expansion of the sections without warpage. The aluminum hood is similarly attached to the top of the frame structure. Upstream of the test section, the frames are closed with 14-gauge aluminum, and also sealed with high-temperature gaskets. The five frames of the test section are fitted with eleven Pyrex windows (two on each frame, and a third window on the last frame, for visual access along the tunnel axis). The window frames may all be opened to gain access to the test section. This feature also allows combustion testing under free-convective flow with air drawn isotropically around the fuel bed. The windows are sealed to their frames, and the frames to the tunnel frame, with silicon-rubber gasketing. They are secured shut with clamps. The windows themselves are 88 cm x 79 cm rectangles for excellent viewing of the combustion event. They are single sheets of 6.4 mm (0.25 in) thick Pyrex.

The movable ceiling is an aluminum plate with rollers that set in a track extending along the entire length of the tunnel. The track is ground smooth and coated with a high-temperature lubricant. A 3 mm (0.125 in) diameter steel cable is attached to the leading edge of the ceiling. The cable is then attached through pulleys to a 5.5:1 gear-ratio winch, which is driven by a 185 W (0.25 hp) electric motor. The motor has a variable-speed drive so that the ceiling can be moved at a rate determined by the operator.

To prevent transmission of vibration to the tunnel, the blower is mounted outside the test facility. It rests on vibration-isolation mounts on a concrete pad separate from the rest of the facility. A rubber duct of 15 cm (6 in) in length isolates the blower from the tunnel and from the building walls.

Because of the large open exhaust area provided for the test section, it seems unlikely that sufficient overpressure to rupture the viewing windows could develop. Consideration of the significant heat loads leads to installation of polycarbonate (lexan) shields just outside the windows. These offer enhanced protection for personnel in the event that a window should fail and burning material should escape from the test section. Fire extinguishers are also provided at personnel test stations.

3.4 Turbulence Suppression

Provision for a low-turbulence, uniform air flow to the combustion zone is necessary for several reasons. Combustion of solids is controlled by transport of oxidant to the vicinity of the solid surface. The rate of transport is altered significantly by the presence of turbulence. Large-scale eddies bring "bubbles" of cool air to the burning region. Smaller-scale disturbances enhance local mass-transfer rates at the burning surface. Experimental repeatability is difficult to establish in flows with large turbulent fluctuations. Development of a one-dimensional flame front does not occur if the wind arriving at the front is nonuniform across the test section width. Similarly, thermal plume development is altered by flow nonuniformities. A coherent plume is not established in sufficiently turbulent flows.

For a satisfactorily uniform flow at the low speeds required up to 8 m/s (18 mi/h), a network of honeycomb, screen and fibrous material is designed for installation upstream of the test section. These measures increase the load on the blower by increasing the pressure drop through the tunnel. For sufficient flow under these conditions, a 45 kW (60 hp) blower capable of providing the required airflow [10.4 m^3/s (22,000 ft^2/min)] through a pressure drop of 3.6 kPa (14 in. water) is selected. Flow-conditioning materials are designed according to the concept of turbulent-scale separation. A honeycomb is provided of cell size roughly one-fifth of the scale of the largest local turbulent structures. A few cell diameters downstream the flow passes through a screen of still smaller mesh size. This process is repeated until the largest remaining scales are small enough to dissipate before reaching the test section. The arrangement of flow-modification devices is shown in figure 3-3. Because of the poor distribution of velocity across the tunnel provided by the blower, 25 cm (10 in) of polyester air-filter material is provided downstream of the largest grid. This provides a region of favorable pressure gradient to aid attachment of the flow to the tunnel walls.

Measurement of turbulence levels in the tunnel was carried out by using a 0.15 mm (0.006 in) diameter hot-film probe operated in the constant-temperature mode. Figure 3-4 shows the air velocity measured by horizontal traverses at three heights above the floor, before and after installation of the flow-conditioning elements. All of the measurements are at the upstream boundary of the test section. The RMS flow turbulence at the test conditions is roughly 3% of the mean velocity. Before modification of the flow, the tunnel radiated noise to the surroundings at about 90 db. The noise dropped an estimated 10 db due to turbulence suppression. The flow is uniform across the test section except near the walls. The higher velocity and turbulence level there are probably caused by air leakage around the edges of the flow-conditioning elements and from flow tripping along the rough walls. It is expected that the viscous wall interaction slows the near-wall flow to a value smaller than the mean velocity as the air progresses through the test section.

3.5 Fuel Matrix Base

Particular attention is devoted to the design and installation of the fuel matrix and base in the test section. A series of trays packed with moist modeling clay are used to support the fuel. The trays span the full tunnel width [1.1 m (44 in)] and length [5.5m (22 in)]. They are 55 cm long so that two trays fill each frame. The five frames composing the test section are filled with ten trays, each containing 14 kg (31 lbm) of clay. Fuel elements are placed in the clay while it is still malleable. Through exposure to ambient air, the moisture evaporates from the clay so that a hard, nonreactive base is left beneath the fuel. The clay is impermeable to air so that oxygen can reach the fuel from the tunnel airflow only. The clay has a flat (not shiny) grey surface, not unlike that of bare earth or urban streets, sidewalks and parking areas. The base accommodates a variety of fuel-element sizes at any desired spacing. Figure 3-5 shows a portion of a fuel tray prepared with wooden fuel elements.

3.6 Ignitor

A propane ignitor is provided for igniting the fuel uniformly along the upwindmost row. The ignitor consists of a 1.3 cm (0.5 in) diameter stainless steel tube held horizontally near the floor of the tunnel just upstream of the upwindmost tray. Holes of 1 mm (0.04 in) diameter are drilled in the tube at 6.4 mm (0.25 in) centers for dispensing the propane. The tube is connected through a solenoid valve to a propane cannister outside the tunnel. A spark transformer provides a high voltage between the tube and a small electrode at one side of the tube about 1.9 cm (0.75 in) away. The transformer and the valve are actuated by a single switch so that, at any time propane is dispensed, the propane is ignited and burned. This procedure prevents the filling of the tunnel with a large quantity of a possibly combustible propane-air mixture. Upon actuation, the flame, stabilized in the airflow by the steel tube, propagates rapidly across the tube length so that ignition is essentially simultaneous across the width of the upwindmost row of the fuel matrix.

3.7 Instrumentation

Data desired from the experiment are the flow conditions upwind of the burning zone (wind speed); the rate, thickness, and shape of the burning front; the effect of the approaching front on the local flow; and the behavior of the thermal plume. To ensure the moving ceiling has not led or driven the plume, data collection must include indication of the leading-edge position of the ceiling relative to the position of the combustion zone.

Measurement of the flame-front propagation speed is accomplished with thermocouples and by image recording and analysis via video cassette recording. Bare chromel-alumel thermocouples formed of 0.1 mm (0.004 in) wire are attached to fuel elements along the axis of the tunnel. Eight thermocouples are spread evenly along the axis at 56 cm (22 in) intervals. The thermocouple wires are wrapped loosely around the elements, so the bead at the thermocouple front surface is left exposed to the oncoming flow (and to radiation from the approaching flame). An individual thermocouple in place on a wooden fuel element is shown in figure 3-6. The thermocouple voltages are stored by strip-chart recorders for later analysis. No reference junction is provided since the temperatures of interest are far above room temperature [100-1000 C (200-1800 F)] . By recording the time lapse for successive thermocouples to reach a fixed temperature, a measurement of the rate of axial flame spread is obtained. Recording of images of the combustion zone with a video cassette recorder (VCR) is also used to measure the flame-spread rate. Sufficient resolution is not available in video recording to record the entire test section in each frame and still to resolve the flame front accurately. The video raster contains roughly 250 lines of resolution. For imaging the entire test section of 5 m in length, one line then corresponds to 2 cm (0.8 in). An uncertainty of ±3 lines in image focusing and recording results in an uncertainty of 12 cm (5 in) in flame-front position. In resolving a bright, rapidly fluctuating flame front in a moderately lit field, considerable degradation in resolution is expected both from local camera overexposure and from motion-induced blurring of the flame-front image. This problem is compounded by use of modern, selfcompensating vidicon color cameras which adjust their sensitivity for the overall field and thereby incur severe overexposure of the combustion-zone image data. These shortcomings are overcome by using five video cameras, one focused on each windowed section of

the tunnel. As the flame traverses the field of each camera, the compensator works to keep the flame image at the correct exposure. The resolution is improved by a factor of five, so that the flame location may be determined with a precision of about 2.4 cm (1 in). A switchbox is used to choose manually which camera video signal is to be fed to the VCR. Digital elapsed time is added to the video signal before it reaches the VCR. This provision gives a continuous time reference printed on each "frame" of the recorded image data. Figure 3-7 shows three of the video cameras at their test positions.

A thermocouple array is also employed to characterize deviation of the flame front from one-dimensionality. Five thermocouples are placed normal to the flow axis at the downstream side of a fuel tray, 2.8 m (110 in) from the leading edge of the fuel matrix. They are positioned along the tunnel floor at the axial centerline and at 20 and 40 cm (8 and 16 in) from the centerline in both directions. Peaking of the thermocouple voltage recorded with strip charts is considered an indication of flame passage. The difference in time of passage of the flame front at the five stations indicates the amount of deviation of the flame front from one-dimensionality.

The effect of the approaching flame on the local airflow is made visible with tufts. A vertical array of doubly-attached tufts is positioned in the center of the test section. Figure 3-8 shows the device which gives a visual indication of flow direction over the total test-section height. The ladder consists of two parallel rods [of diameter 1.6 mm (1/16 in)] spanned by gold- and aluminum-coated kapton strips. The strips billow in either the upstream or the downstream direction, according to the local wind. They are sensitive to wind speeds less than 0.1 m/s (0.2 mi/h). Additional kapton tufts are attached to identical rod segments, positioned within the fuel matrix and standing 1 cm (0.4 in) taller than the fuel elements. These indicate the direction of airflow at various positions relative to the combustion zone.

For recording the position of the leading edge of the ceiling for later correlation with flame-front position, a ceiling-indicator device is provided. A 454 g (16 oz) magnet is attached to the ceiling leading edge, which is inside the exhaust hood. An iron washer outside the hood is held by the magnet so that, as the ceiling is drawn forward, the magnet moves with it. A red ribbon attached to the washer hangs down into the video camera field of view so that the flame and ceiling positions are recorded simultaneously.

Fur er documentation of the test is provided with two 35 mm still cameras d a 16 mm movie camera. One of the 35 mm cameras is handheld to permit s ection of pictures of interest as the test progresses. The camera is used rticularly to record tuft behavior as the flame approaches. The other 35 m camera is fixed at an angle to the tunnel so that sequential pictures re taken from a fixed location as the flame propagates. The 16 mm movie ca ra has sufficient resolution to image the entire test section from an angle o provide qualitative data on flame behavior and propagation. It is operated t 24 frames per second.

4 EXPERIMENTAL RESULTS

Trials using single fuel trays were carried out for a variety of wooden fuel-element shapes and loadings over a range of wind speed. These tests also verified the viability of a clay base for the fuel trays. A wind speed of 1.37 m/s (4.5 ft/s) was selected for the multitray tests on the basis of tunnel-sizing calculations of section 3 and of the propagation rates observed during the trials. The RMS turbulence level at this speed was 3.0% of the mean velocity (see figure 3-4 for the flow profile present for the tests). Two fuel types were selected for the inital multitray tests on the basis of their ability to propagate flame easily.

4.1 First Test

For the first test, flat, hardwood toothpicks were spaced axially and transversely on 1.27 cm (0.5 in) centers. The fuel elements were of length 5.84 cm (2.3 in), of which 5.52 cm (2.2 in) extended above the clay surface. The exposed surface was 2.99 cm^2 (0.46 in^2) and the mass above the clay was 53 mg, so that each element had a surface-to-mass ratio of 5.64 m^2/kg (27.6 ft^2/lbm). The loading of exposed fuel (not submerged in clay) was 0.321 kg/m^2 (0.066 lbm/ft^2). Figure 3-8 shows the fuel matrix in place in the tunnel. No sticks were placed on either tray edge within 10 cm (4 in) of a tunnel wall. This limits the amount of flame propagation taking place in the boundary layer, where the velocity field is nonuniform. By keeping the burning region away from the windows, the heat loading on the glass is reduced. The fuel-free zone was purposely made only half as wide as the expected boundary layer because of wall-quench-layer considerations. The absence of burning elements and their contribution to convective and radiative heating at one side of the outside columns of fuel elements is expected to slow combustion and flame propagation near the walls. By providing fuel outside of the uniform-flow corridor, it is possible to mitigate this effect within the corridor. The portion of the fuel which is retarded by viscous boundary-layer effects is in effect used to absorb thermal-quench-layer effects. This compensation is imperfect because combustion in this compensative region does not keep pace with the rest of the flame front. Nonetheless it does aid in insulating the region outside the wall boundary layer from the cold walls.

Figure 4-1 shows the flame development sequentially. Figure 4-1a shows the flame front after the ignitor was extinguished. The front is narrow with only slow burning. The very flat (horizontal) plume is expected because, during the starting transient, convective strength has not yet developed and the plume is blown over by the wind. As the flame approaches steady state (figure 4-1b) the combustion zone widens and the plume becomes slightly inclined toward the vertical. The ceiling-leading-edge indicator is the red ribbon hanging into the field of view of the first window. The outer frames visible in this view hold the polycarbonate protective windows discussed in section 3. The flow-direction indicator is visible in figure 4-1c. It shows a strong streamwise pattern over the upper half of the test section, with backflow and areas of forward flow in the lower half. A single tuft, positioned just above the fuel elements at a site 50 cm (22 in) downwind of the indicator, shows weak backflow. This general pattern continues through figure 4-1g,although, as the flame approaches, the backflow appears to weaken, so that in figure 4-1h only forward flow is observed. The two dimensionality of the burning zone is apparent in figure 4-1k. The flame has consumed the fuel along the centerline at the center of the third window from the upwind end of the test section; however, strong burning is still occurring along the edges. The flame width is determined by measuring the length of burning along the centerline of the fuel bed. The curved combustion region shape remains through figure 4-1l. The test ends when the leading edge of the flame front reaches the end of the last fuel tray, as depicted in figure 4-1l. Approximately 70 seconds of elapsed time is depicted in this sequence.

A portion of the fuel bed after the test is shown in figure 4-2. The fuel in the center of the matrix is almost completely burned. At the upper right-hand side of the figure, a few fuel elements which were only partly burned are visible. Small groups of such partially burned fuel elements remained in several areas along the outer edges of the matrix.

4.2 Second Test

The tunnel was prepared for the second test by replacing the fuel trays with fresh trays packed with the second set of fuel elements. These elements were hardwood sticks similar to Popsicle sticks. They are 11.4 cm (4.5 in) in length, of which 11.1 cm (4.37 in) extended above the clay surface. The

elements had an exposed surface area of 27.0 cm^2 (4.2 in^2) and an exposed mass of 1505 mg (0.003 lbm), so that the fuel-element surface-to-mass ratio was 1.79 m^2/kg (4.57 ft^2/lbm). The fuel matrix was formed of elements spaced at 1.27 cm (0.5 in) centers in the streamwise direction and at 2.5 cm (1 in) centers in the transverse direction. The loading of the exposed fuel for this geometry is 4.77 kg/m^2 (0.975 lbm/ft^2), almost 15 times greater than that of the first test. A portion of the installed fuel matrix is shown in figure 4-3. Leaning of a small number of fuel elements was not considered significant to flame propagation through a matrix of a large number of elements. In this case, the matrix was composed of 35 columns and 387 rows totaling over 13,500 discrete elements. As in the first test, the 10 cm (4 in) nearest to the walls on both sides of the tunnel were left free of fuel elements to avoid boundary-layer effects and to lighten the heat load on the windows.

Figure 4-4 shows the flame propagation and development for this test. The initial burning zone is narrow and one-dimensional (figure 4-4a) and the plume appears nearly horizontal. A more vertical plume begins to arise as the burning region increases to roughly 50 cm in thickness (figure 4-4b), and the plume clearly is nearly vertical in figure 4-4c. The flame continues to grow in width (figure 4-4d) without reaching a steady state within the length of the test section.

4.3 Test Results

Primary determination of the flame-front location and its rate of progress is by temperature measurements made with the thermocouples in the fuel bed. Since the recorded temperature monotonically rises, and then monotonically falls with the passage of the combustion zone, it is necessary to identify the flame front with a particular threshold temperature. Figure 4-5 shows the position of the flame determined with this threshold technique applied at two temperatures, 685 K and 1120 K, for the first test. The rate of propagation is found to be quite constant along the length of the tunnel. The particular temperature chosen effects only a horizontal shift in the curve and does not significantly alter the estimate of the flame-propagation rate. This rate, found by least-squares fitting to the data, was 7.0 cm/s. The correlation coefficients for the fits were 0.997 or better, an indication of

)nstant flame-propagation rate. The ceiling position is also plotted to show)w the leading edge followed the flame front. At time t=37 s, the ceiling :gan to lag the flame front by a greater distance than earlier. The earlier ıg was recovered at time t=65 s. Significantly, the flame propagation)pears unaffected by small variation in the lag distance of the ceiling. ıis indicates that the ceiling position was not driving the propagation. VCR ıage data was also used to measure flame-propagation rate. The image data, ıich contain time reference, were examined manually at intervals of :n-to-fifteen seconds of elapsed burning time and the flame-leading-edge)stion was recorded. The consistency of the image data with ıermocouple-derived data supports the determination of extremely constant ame propagation at 7.0 cm/s. Figure 4-6 shows a single video frame. The ıy (013) and precise time, shown at the upper left-hand corner, is included ı each image on the video record. While the leading edge of the flame is early visible, the limited resolution and particularly the limited dynamic ınge of the video camera make it difficult to determine whether the flame :ading edge shown is actually a site of burning sticks or just a tongue of ırning gas blown forward from the true flame front. For this reason and :cause of the need for manual determination of the flame-front position, the deo technique was considered inferior to the thermocouple measurements.

Video and film image data showed clearly that while the flame-front opagation was steady, the flame front was far from one-dimensional during ıe first test. This observation is confirmed by figure 4-7 which presents ıe elapsed time to reach particular temperatures at five positions in the ıel array. These positions are all at the same distance downstream [279 cm 110 in)] from the fuel-bed leading edge, but at transverse positions ±20 cm 3 in) and ±40 cm (16 in) from the axial centerline, as well as at the :nterline. Each thermocouple reading was normalized by its peak reading ırıng flame passage. The lines connecting the data points indicate the times : which each thermocouple reached its peak reading and its half-peak reading)th during the heating (flame-approaching) and cooling (flame-leaving) ıases. The lateral lag in the flame-front position decreases from 16 seconds ırıng the flame-approaching phase, to only 9 seconds during the flame-leaving ıase; this difference indicates that the nonlinearity was actually decreasing ; the flame propagated. The nine-second lag corresponds to a variation in lame location of 63 cm (25 in).

The modified plume-dynamics-controlled flame-propagation theory of G.I. Taylor for a line fire in a crosswind (Taylor 1961; Carrier et al 1984a) was compared with the present results and with results of burns carried out in the Canadian National Forest (Brian Stocks, Great Lakes Forest Research Center, private communication). The theory allows calculation of the rate of flame propagation v, from knowledge of the windspeed u and fuel loading σ and exothermicity Q, via the relation

$$v = \frac{\rho_a c_p T_a u^3}{8\alpha^2 g Q \sigma} \quad . \tag{4-1}$$

For both the forest-fire data of Stocks and the present data, the ambient air density ρ_a is taken to be 1.1 kg/m^3; the specific heat capacity of air c_p, 1.004 kJ/kg-K; the ambient temperature T_a, 300 K; the magnitude of the gravitational acceleration g, 9.8 m/s^2; and the exothermicity of the fuel Q, 18,570 kJ/kg. The entrainment factor α is computed from

$$\alpha = 0.16 \, (\rho_{fire}/\rho_a)^{\frac{1}{2}}$$

$$= 0.16 \, (T_a/T_{fire})^{\frac{1}{2}} \quad .$$

The "fire temperature" is taken at the approximate pyrolysis temperature of the fuel (as recommended by Carrier et al 1984),roughly 675 K. For the laboratory tests, the wind speed u was 1.37 m/s (4.5 ft/s) and the fuel loading σ was 0.321 kg/m^2. The calculated flame velocity for the laboratory test is 16 cm/s (6.3 in/s), a factor of 2.3 greater than the measured 7 cm/s (2.76 in/s). For the forest-fire data, the wind speed was 6.7 m/s (22 ft/s) and the fuel loading was 3.0 kg/m^2, for a calculated flame velocity of 201 cm/s (79 in/s). The value measured by Stocks was 110 cm/s (43 in/s). While neither calculation indicates that (4-1) result might have predictive power on its own, the calculations both suffer from roughly the same fractional error compared to experiment. This indicates that experimental measurement could yield a factor by which (4-1) might be multiplied. The equation might then have predictive power for wind-aided fire spread. In the present examples, the correction factor indicated is 0.44 for the laboratory data and 0.55 for the field results. Thus a factor of 0.5 correlates the results of both tests

within roughly a ±10% error bound. This is encouraging, since the two tests are in many ways near antipodes of physically interesting parametric ranges. The forest data was acquired at nine times the fuel loading, and almost five times the wind speed, of the lab test. The size scales of the fuel elements range over almost three orders of magnitude (between trees in the forest and 5 cm fuel elements in the lab test). The remaining error is attributable to uncertainties in the fuel-loading data for the forest, for which an estimate of fuel thin enough to participate in the flame propagation must be made. Exothermicity is also not well known for either case, since corrections (e.g., for relative humidity and for specific wood type) have not been applied. The flame-spread wind tunnel permits an order-of-magnitude variation in wind speed and fuel loading, so that tests over a wide range of these parameters could be conducted to evaluate further the adequacy of (4-1)for correlating experimental data.

5. OTHER UTILIZATIONS OF THE FIRE-RESEARCH FACILITY

5.1 Fire Merger

A relatively modest variation on fire spread across a regular two-dimensional array of discrete fuel elements may be carried in the fire-research facility to examine the capacity of fires from initially isolated ignitions to merge, and to identify the time scale (if merger does occur). These tests are envisioned to involve three-dimensional cribs (possibly, Tinker-Toy-like arrangements of wooden sticks, to permit inexpensive reproducibility in size, weight, and detail of the initial fuel distribution); while some use of the fan to produce a wind may be entailed, the preponderance of the experiments would be conducted with the fan turned off.

Ignition sites are to be symmetrically located among the discrete cribs. The cellular yet dispersed nature of the nonhomogeneous fuel distribution achieved by use of multiple cribs in orderly arrangement gives a well-defined experiment that still recovers the strewn-debris nature of a blasted urban environment. The firebreaks afforded by parks, rivers, expressways, etc., in cities are simulated by adopted separation of the block-type crib fuel loading. The ability of air to flow into the streets between the cribs, in face of the strong convection, is of central interest; such influx is crucial if fuel distributed over a large area is to be simultaneously burning.

It is the essence of the test that only some of the cribs are lighted; the capacity of the remaining cribs to ignite (and on what time scale) is the key information sought. Radiative transfer is the principal mechanism for heat transfer to the initially unlighted cribs in the absence of an applied wind. If the fan is turned on, then the upwindmost (or downwindmost) cribs are ignited; for wind-aided arrangement, spread by contact ignition may enter.

The very tall duct with unforced exhaust, such that the strongly buoyant plume is not artificially constrained by a ceiling of the housing structure, is seen to be a critical asset of the fire-facility design.

5.2 Enhanced Entrainment into the Burning Zone of a Buoyant Plume

Whereas the fire-merger experiments just mentioned involve little more than proceeding from two-dimensional to three-dimensional fuel distributions

(and to altering the ignition provisions), elucidation of the previously discussed phenomenon of appreciably enhanced induction of air into the low-altitude, flaming domain of a fire plume requires more extensive modification of the facility. However, in common with fire merger, the questions involved do concern nonhomogeneity of the fuel distribution, and in general are to be carried out in the absence of an applied wind.

In a large fire over common polymeric fuels, over a height of several hundred feet from the ground (but below the completion-of-burning altitude), perhaps five-to-ten times the stoichiometric amount of air is added to the rising pyrolyzate combustible vapor (released via thermal degradation of the solid fuel at ground level). Because of the modest updraft speeds near the ground, this entrainment is readily perceived to be many times that predicted by classical entrainment theory, which does describe accurately the relatively modest level of ambient-air addition into the weakly buoyant plume above the completion-of-burning plane.

It is suggested that there is a cellularity to the low-level burning, though the cells merge to form a single plume entity above the completion-of-burning plane. This cellularity arises partly from any nonuniformity of the fuel distribution and of radiative transfer from the flames above to the fuel below. If there is roughly neutral vertical stability over the modest altitude of the fire zone (from ground plane to completion-of-burning plane), then the cellularity implies large-scale overturning and a high degree of unmixedness. The large-scale nonuniformity of the burning domain results in the need for much excess air to effect combustion. It seems worth noting that transverse gradients are lost in transverse averaging, but in fact large density gradients at interfaces between hot product gas and cold reactants exist. In short, simplistic treatment could overlook the cellularity.

If cellularity did not permit enhanced low-level influx of ambient air into the burning region, the center of a large burning region would be oxygen-starved; while the peripheral fuel might be converted to product gas in an annular burning, the central fuel would not be converted except possibly at great height (and

even in the Hamburg firestorm there were no reports of flames persisting more than one kilometer above the ground.

The above-stated suggestion that the fire zone is roughly neutrally stable implies that it is approximately isothermal. The level of air entrainment needed to maintain an isothermal burning zone in face of the exothermicity associated with chemical conversion of the fuel vapor depends upon the temperature at which the fuel vapor is issued. The entrainment (i.e., dilution) consistent with isothermal conditions increases as the pyrolysis temperature of the polymeric solid fuel decreases; the dilution requirement becomes indefinitely large for fuel vapor issuing (from pipes) at room temperature. This statement assumes comparable rate of fuel-vapor mass "injection" and comparable exothermicity from combustion for fuels of interest.

Accordingly, one may wish to work with wood cribs or slabs ("pools") of cellular plastics or clusters of identical gaseous-hydrocarbon-emitting pipes, though in the last-mentioned case the fuel vapor must issue at a modest flow rate consistent with buoyancy control (as distinct from forced-convection control). *In any case, it is the clustering of the fuel distribution that is of* interest: increased burning-region perimeter is postulated to incur increased entrainment, as the same mass of fuel is distributed in more and more discrete "pools." The separation between clusters should be conservatively on the order of the "equivalent radius" of a cluster, to ensure that two clusters are not merged; clearly the limiting separation is to be sought by testing.

Segregating fuels into ever smaller "pools" does not assure ever increased entrainment of ambient air into the plume. A limit is furnished by the inviscid Bernoulli relation between radial influx and lateral (nonhydrostatic) pressure discrepancy. It is unclear that this limit can be reached feasibly in a laboratory-scale experiment. In any case, if one has one single "cluster" or "pool", one should entrain less air, and should observe a greater flame height, than if one disperses the cluster or pool in many segments. Elsewhere (Carrier et al 1984b) it has been conjectured that the increase in entrainment goes as the square root of the number of clusters (until the inviscid limit).

While the sidewalls of the fire apparatus as set up for wind-aided flame spread experiments would have to be removed for the entrainment experiment, and the floor of the test section laterally extended, still the essential ingredient of a large, tall duct to permit unconstrained convective ascent has been provided. It seems worth mentioning that comparing cases, rather than absolute measurement, suffices to indicate enhanced induction, and hence enhanced upflux. Thus, introduction of sophisticated rakes of thermocouples and anemometers in the duct is not required; simply correlated deflection of pennants suspended on horizontal wire, or inflection of a narrow-mesh net constituting the lateral face of a right-circular cylinder enveloping the fuel-issuing region, could be used.

This discussion seems sufficient to suggest the utility of the laboratory fire facility (with minor modification) in many contexts pertinent to large-scale incendiary effects of large weapons.

REFERENCES

Broido, A. (1960). Mass fires following nuclear attack. Bull. Atomic Scientists 16, 409-413.

Brunswig, H. (1982). Feuersturm über Hamburg. Stuttgart, West Germany: Motorbuch Verlag.

Caidin, M. (1960). A Torch to the Enemy: the Fire Raid on Tokyo. New York, NY: Ballantine.

Carrier, G. F., Fendell, F. E., and Feldman, P. S. (1983). Firestorms. Fire Dynamics and Heat Transfer, 55-64. Heat Transfer Div., v. 25. New York, NY: Amer. Soc. Mech. Engineers.

Carrier, G. F., Fendell, F. E., and Feldman, P. S. (1984a). Studies in urban-scale-fire thermohydrodynamics. Rept. 42132-6001-UT-00. Redondo Beach, CA: TRW Electronics and Defense Sector.

Carrier, G. F., Fendell, F. E., and Feldman, P. S. (1984b). Big fires. Combust. Sci. & Tech., to appear.

Cate, J. L., and Craven, W. F., eds. (1953). The Army Air Forces in World War II. Vol. 5: The Pacific--Matterhorn to Nagasaki, June 1944 to August 1945. Chicago, IL: U. Chicago.

Cox, G., and Chitty, R. (1980). A study of the deterministic properties of unburned fire plumes. Combust. & Flame 39, 191-209.

FitzGibbon, C. (1957). The Winter of the Bomb--The Story of the Blitz of London. New York, NY: W. W. Norton.

Futrell, R. F., Moseley, L. S., and Simpson, A. F. (1961). The United States Air Force in Korea, 1950-1953. New York, NY: Duell, Sloan & Pearce.

Glasstone, S., and Dolan, P. J., eds. (1977). The Effects of Nuclear Weapons, 3rd ed. Washington, D.C.: U.S. Dept. of Defense & Dept. of Energy.

Irving, D. (1965). The Destruction of Dresden. New York, NY: Ballantine.

Pyne, S. (1982). Fire in America. Princeton, NJ: Princeton U.

Rouse, H. (1947). Gravitational diffusion from a line source in two-dimensional flow. J. Appl. Mech. 14, A225-A228.

Taylor, G. I. (1961). Fire under the influence of natural convection. International Symposium on the Use of Models in Fire Research, 10-28. Washington, DC: National Academy of Sciences National Research Council (Publication 786).

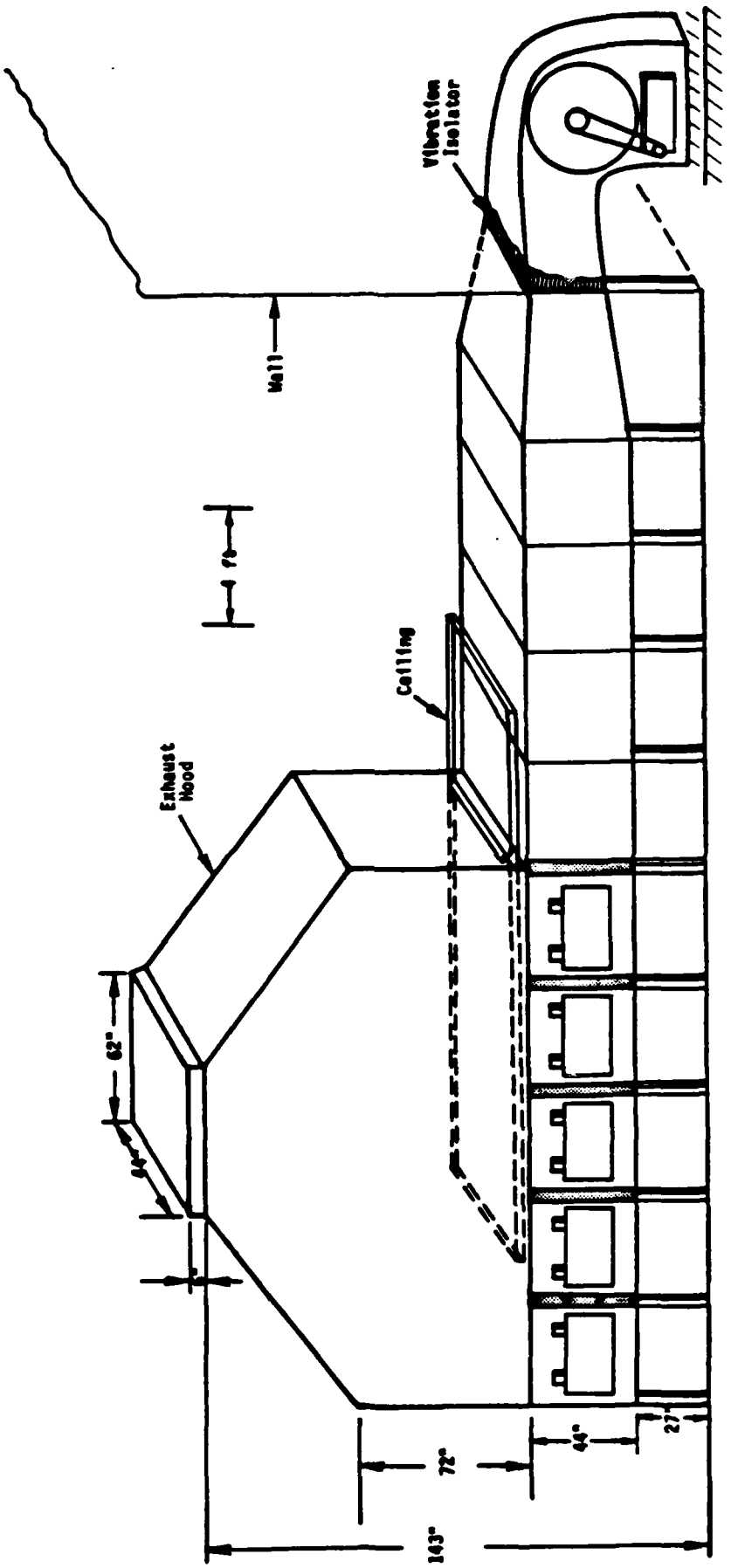

Figure 3-1. Schematic diagram of the flame-spread wind tunnel.

Figure 3-1. The flame-spread wind tunnel installed at TRW. The blower inlet is through the wall at the right side of the figure. All window panes may be fully opened for test-section access. A portion of the movable ceiling panel is visible above the inlet sections.

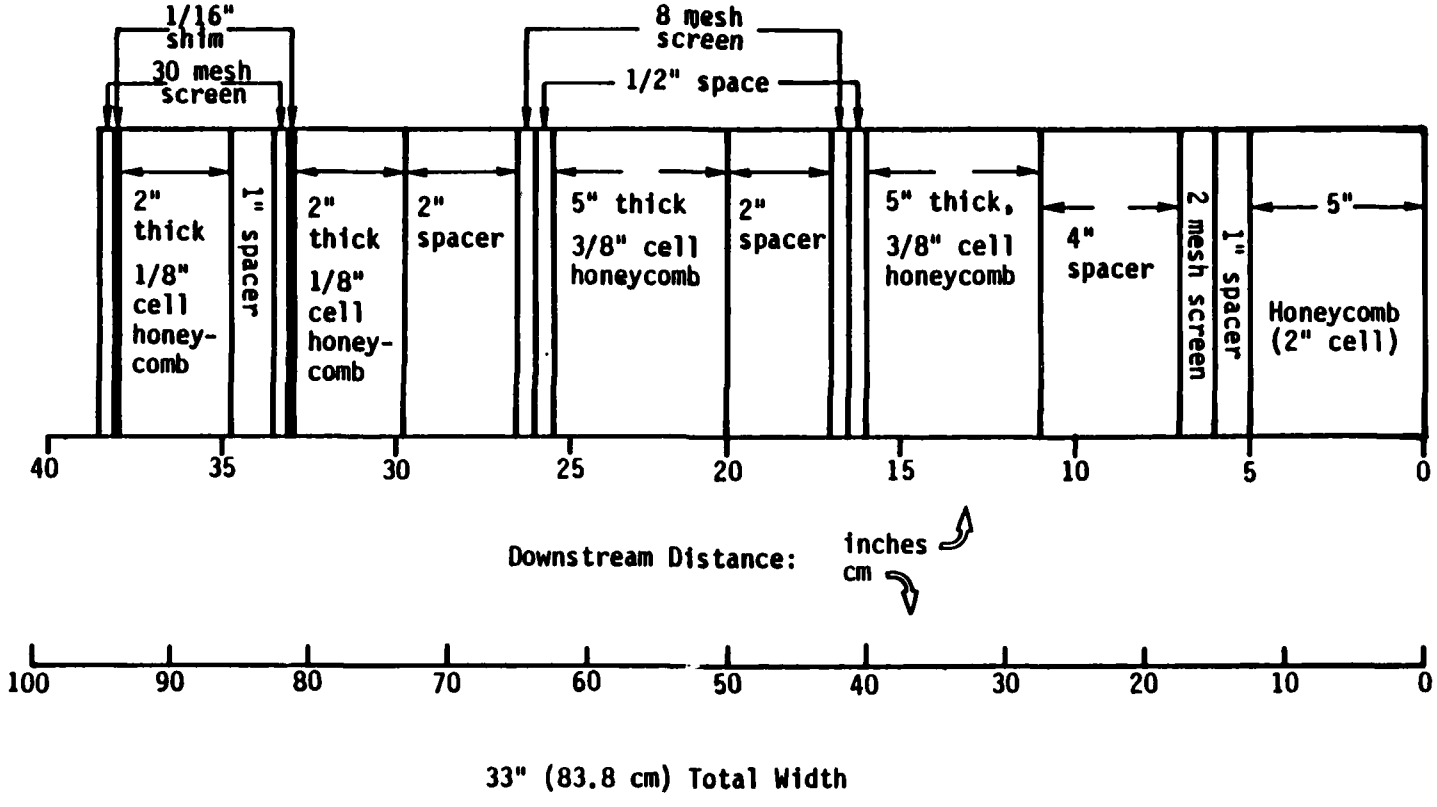

Figure 3-3. Arrangement of flow-conditioning elements in the wind-tunnel inlet section. The last flow-conditioning element is 2.2 m upstream of the test section, to allow "imprints" of the elements on the airflow to dissipate.

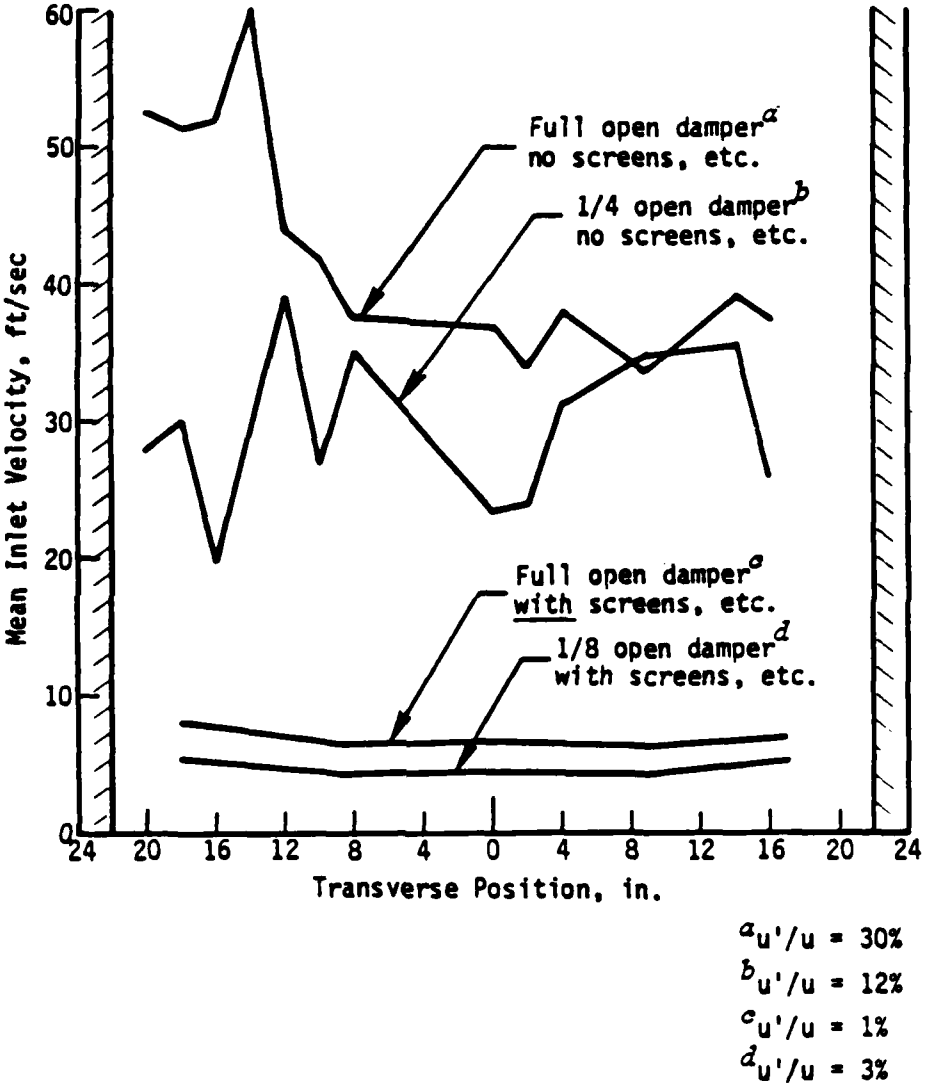

Figure 3-4. Hot-film measurements of the streamwise air speed in the tunnel. Transverse traverses shown are 59 cm (22 in) above the tunnel floor. Configuration d was used for all flame-spread tests. These measurements are at sites 279.4 cm (110 in) from the leading edge of the test section.

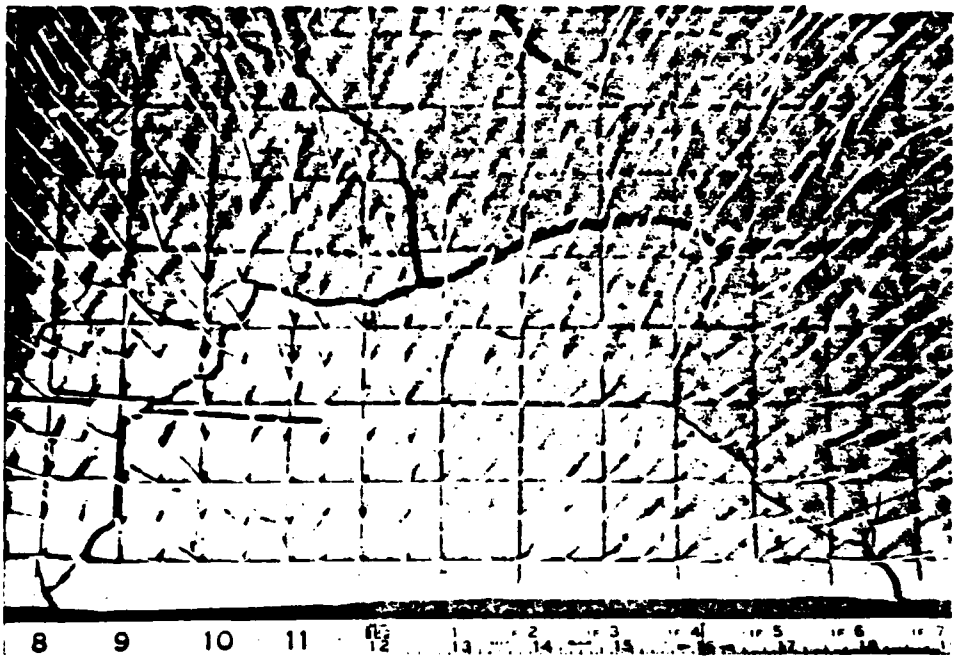

Figure 3-5. A portion of a fuel tray photographed from above. The tray is packed with 5 cm (2 in) flat hardwood sticks on 1.27 cm (½ in) centers. The cracks in the clay surface result from drying in thin areas and has been considerably reduced from that shown. The flame-propagation data of Section 4 are for this fuel and configuration.

Figure 3-6. A thermocouple mounted on the forward-facing side of a 5 cm (2 in) hardwood stick.

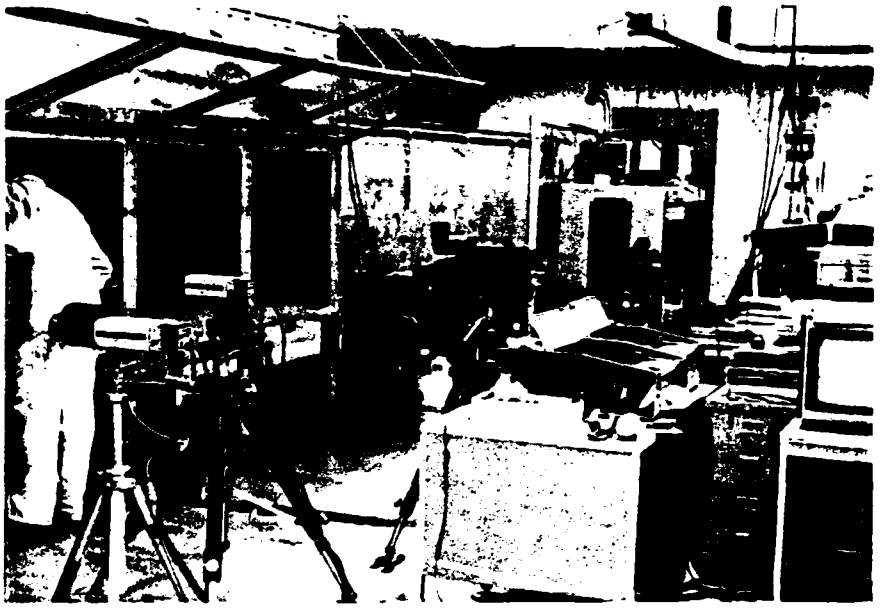

Figure 3-7. Four of the five video cameras for recording flame and plume images are visible in this photo (arrows). An operator selects the video signal to be recorded from the view shown on the monitor (far right). Thermocouple strip-chart recorders are left of the monitor.

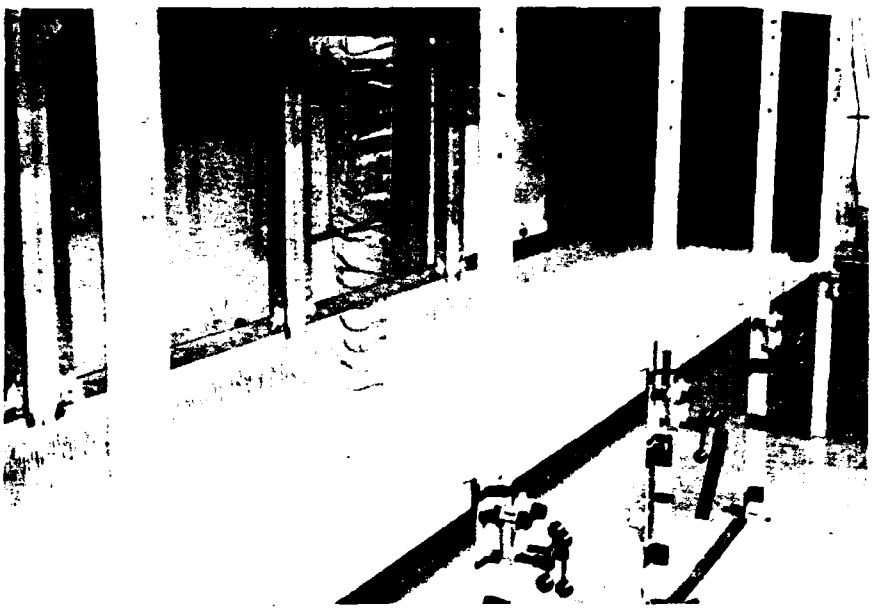

Figure 3-8. The flow-direction indicator installed above a fuel matrix ready for the test.

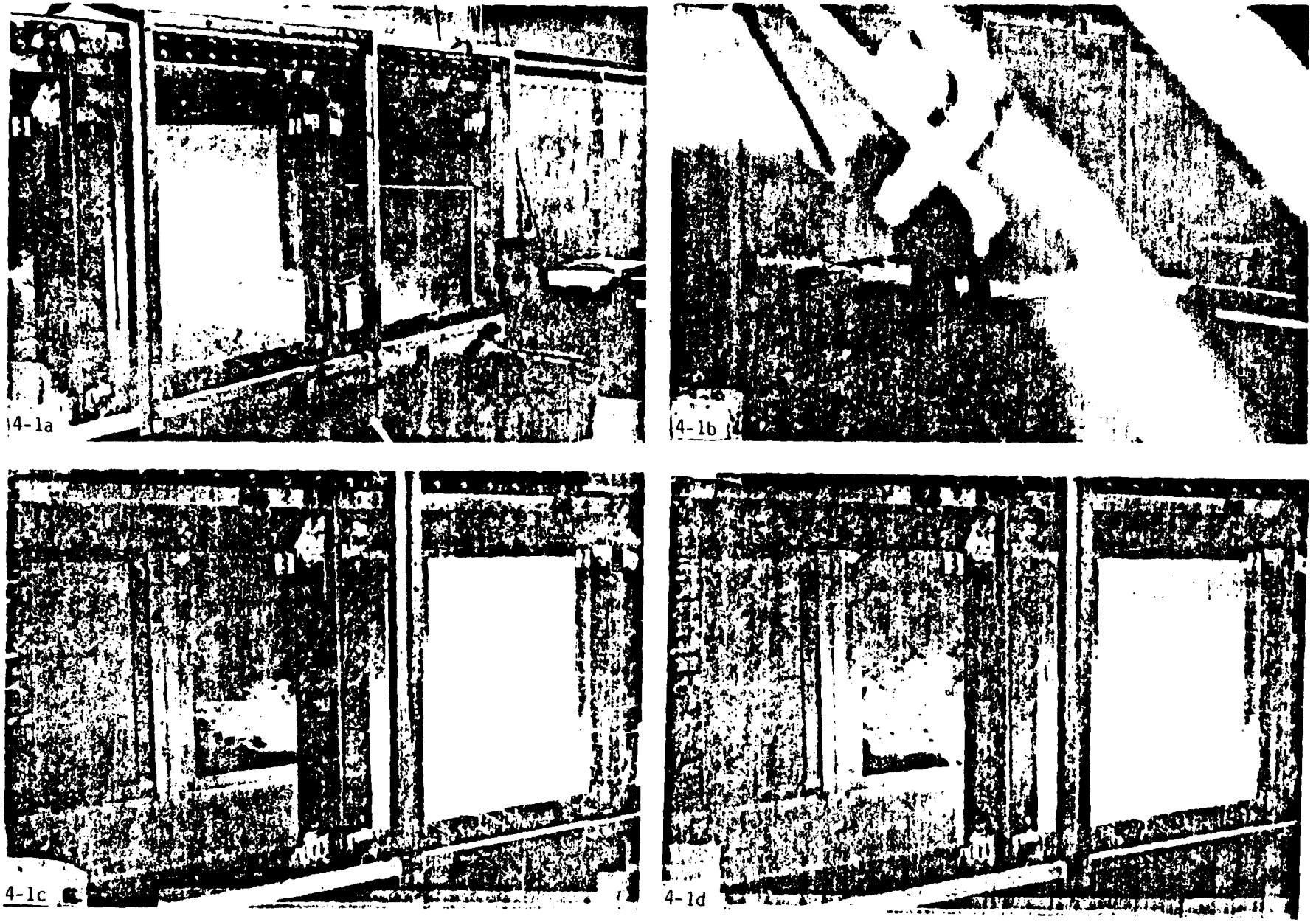

Figure 4-1. Flame spread over a fuel bed composed of flat hardwood sticks. Fuel loading 0.321 kg/m^2; windspeed 1.37 m/s (4.5 ft/s).

4-1e

4-1f

4-1g

4-1h

Figure 4-1. (Continued)

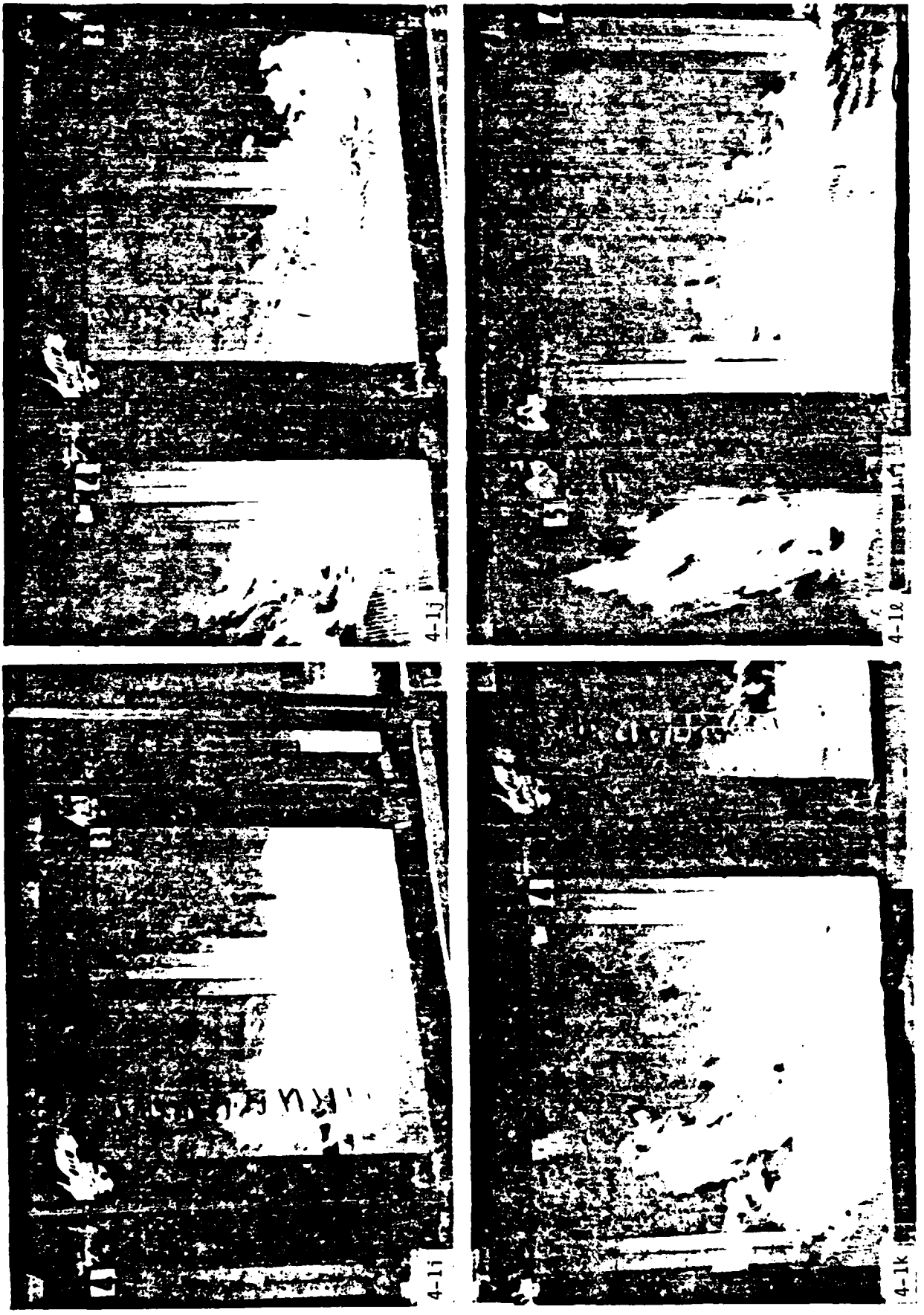

Figure 4-1. (Continued)

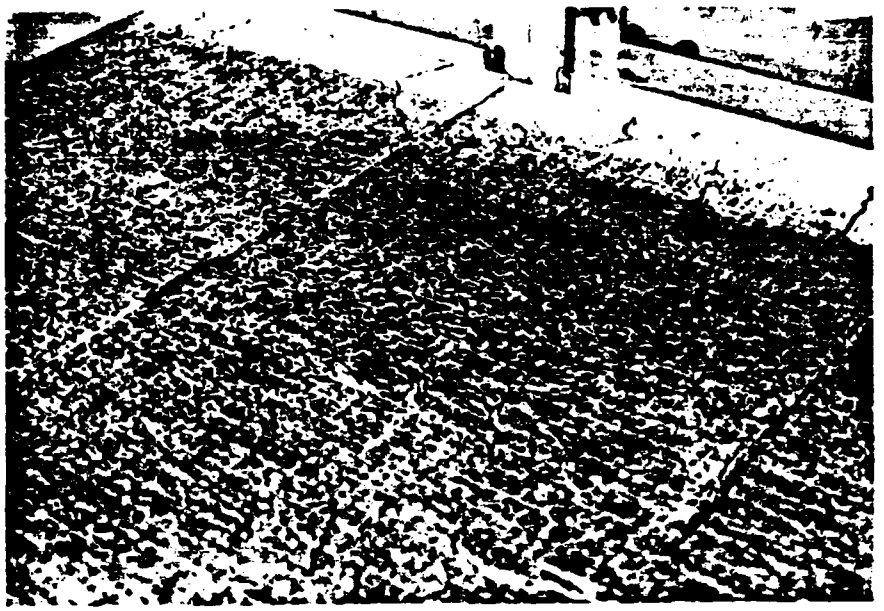

Figure 4-2. The fuel base after test. Partially burned fuel elements are visible at the upper right.

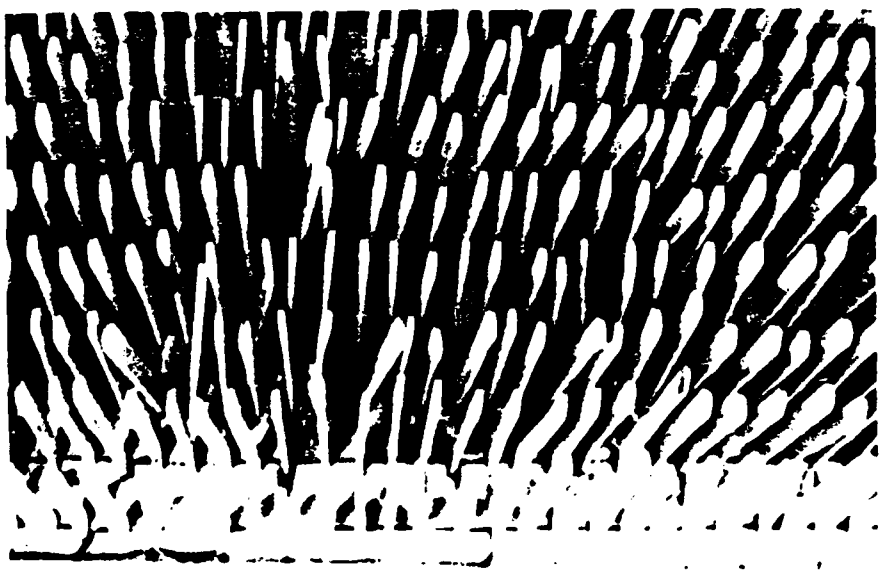

Figure 4-3. The fuel matrix prepared for the second test. Fuel loading 4.77 kg/m^2.

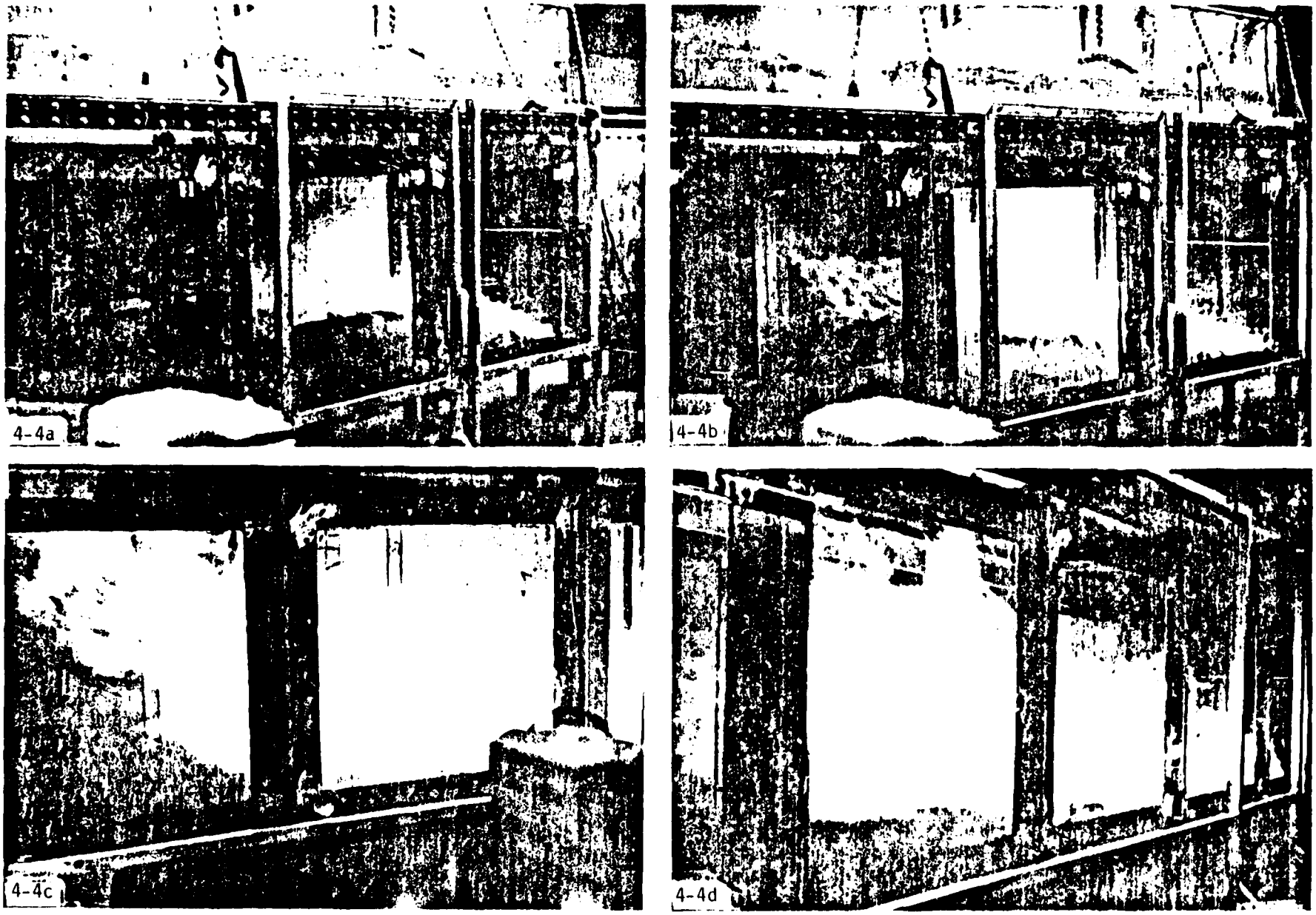

Figure 4-4. Flame spread over a fuel bed of loading 4.77 kg/m². The wind speed is 1.37 m/s (4.5 ft/s).

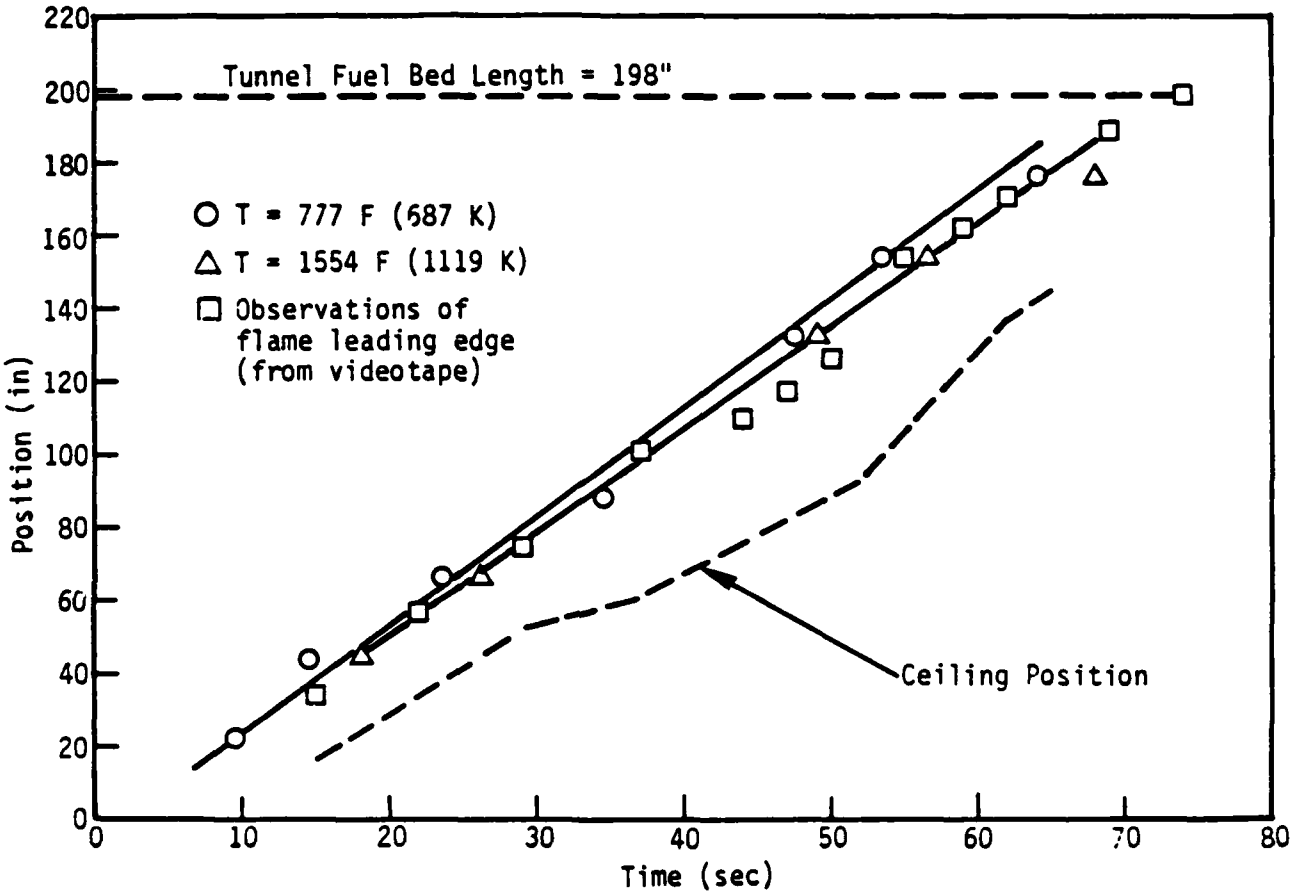

Figure 4-5. Flame position as a function of time as measured with thermocouples (,) and visual data ( ), for test with flat toothpicks and wind speed 1.37 m/s (4.5 ft/s).

Figure 4-6. Single frame of video data. Test date and real time are displayed at the upper left.

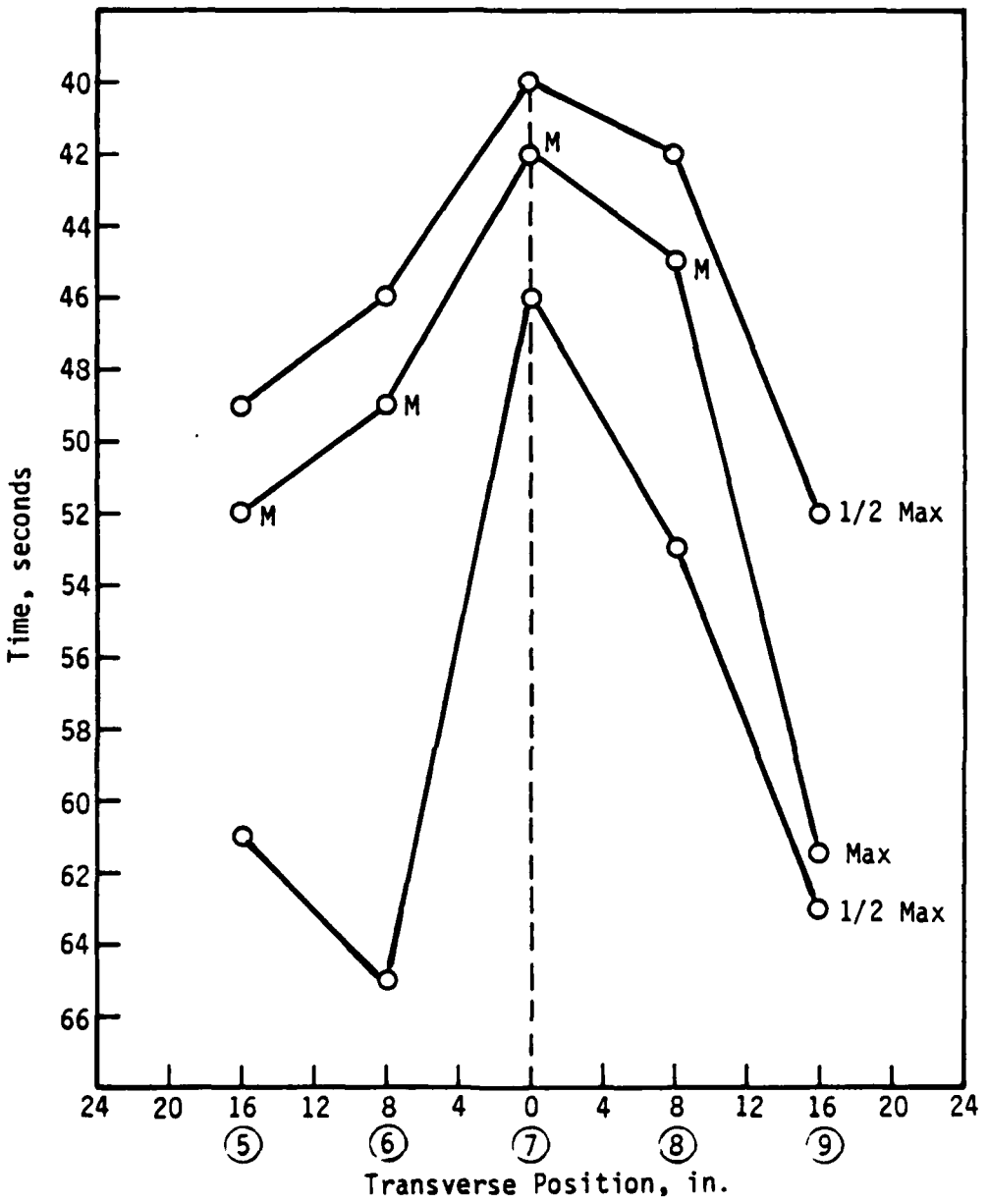

Figure 4-7. Temporal isothermal map shows the retardation of the flame front away from the tunner centerline. These measurements are at sited 279.4 cm (110 in) from the leading edge of the test section.

DISTRIBUTION LIST

DEPARTMENT OF DEFENSE

Defense Intelligence Agency
ATTN: DB-4C2, C. Wiehle
ATTN: WDB-4CR

Defense Nuclear Agency
ATTN: STSP
2 cys ATTN: SPTD
4 cys ATTN: STTI-CA

Field Command, Defense Nuclear Agency
ATTN: FCTT, W. Summa
ATTN: FCTXE

Joint Strat Tgt Planning Staff
ATTN: JLKS

OTHER GOVERNMENT AGENCIES

Dept of Commerce, Ctr for Fire Rsch
ATTN: R. Levine
ATTN: H. Baum
ATTN: G. Mullholland
ATTN: J. Quintierre

US Forest Service
ATTN: C. Chandler

Federal Emergency Mgmt Agency
ATTN: Asst Assoc Dir for Rsch, J. Kerr
ATTN: Ofc of Rsch/NP, D. Bensen
ATTN: H. Tovey

Office of Emergency Services
ATTN: W. Tonguet

FOREIGN AGENCY

Great Lakes Forest Research Ctr
ATTN: B. Stokes

DEPARTMENT OF ENERGY CONTRACTORS

University of California
Lawrence Livermore National Lab
ATTN: B. Bowman
ATTN: R. Hickman
ATTN: R. Perrett

Los Alamos National Laboratory
ATTN: J. Chapiak
ATTN: Dr D. Cagliostro

DEPARTMENT OF DEFENSE CONTRACTORS

Science Applications, Inc
ATTN: M. Drake
ATTN: M. McKay
ATTN: D. Groce

Scientific Services, Inc
ATTN: C. Wilton

Stan Martin Associates
ATTN: S. Martin

DEPARTMENT OF DEFENSE CONTRACTORS (Continued

California Research & Technology, Inc
ATTN: M. Rosenblatt

Carpenter Research Corp
ATTN: H. Carpenter

Center for Planning & Rsch, Inc
ATTN: J. Rempel
ATTN: R. Laurino

Charles Scawthorn
ATTN: C. Scawthorn

Factory Mutual Research Corp
ATTN: J. DeRis
ATTN: R. Friedman

Harvard University
ATTN: Prof G. Carrier

IIT Research Institute
ATTN: T. Waterman
ATTN: H. Napadensky
ATTN: A. Longnow

Institute for Defense Analyses
ATTN: L. Schmidt
ATTN: E. Bauer

Kaman Sciences Corp
ATTN: E. Conrad

Kaman Tempo
ATTN: DASIAC

Kaman Tempo
ATTN: DASIAC

Los Alamos Tech Associates, Inc
ATTN: P. Hughes

University of Notre Dam du Lac
ATTN: A. Murty Kanury

Pacific-Sierra Research Corp
ATTN: H. Brode, Chairman SAGE
ATTN: R. Small

R&D Associates
ATTN: F. Gilmore
ATTN: R. Turco
ATTN: D. Holliday
ATTN: P. Haas

Rand Corp
ATTN: B. Bennett

Rand Corp
ATTN: P. Davis

Research Triangle Institute
ATTN: R. Frank

Science Applications, Inc
ATTN: J. Cockayne

DEPARTMENT OF DEFENSE CONTRACTORS (Continued)

SRI International
ATTN: J. Backovsky
ATTN: T. Goodale
ATTN: R. Alger

SWETL, Inc
ATTN: T. Palmer

DEPARTMENT OF DEFENSE CONTRACTORS (Continued)

TRW Electronics & Defense Sector
ATTN: P. Feldman
2 cys ATTN: F. Fendell
2 cys ATTN: G. Carrier
2 cys ATTN: R. Fleeter
2 cys ATTN: N. Gat
2 cys ATTN: L. Cohen

END

FILMED

5-85

DTIC